CrossMark

RESEARCH PAPER

Effects of HAZ widths on creep crack growth properties of welded joints

G. Chen[1] · G. Z. Wang[1] · F. Z. Xuan[1] · S. T. Tu[1]

Abstract The finite element method (FEM) based on ductility exhaustion damage model was used to investigate the effects of heat-affected zone (HAZ) widths on creep crack growth (CCG) properties for the compact tension (CT) specimens with pre-crack located in the middle of softer and harder HAZs under the same initial load level. The results show for the welded joints with softer HAZ containing crack that the creep rupture life increases and CCG rate decreases with increasing HAZ width due to the decrease of material constraint effect. For the welded joints with harder HAZ containing crack, a second crack in soft material near interface generally forms, and the rupture life is mainly determined by the initiation time of the second crack. The CCG length in harder HAZ increases with increasing HAZ width. There exist proper widths of the harder HAZ which have the longest rupture life due to the lower stress triaxiality and later initiation of second crack in soft material near interface. The CCG properties of HAZs may be improved by adjusting HAZ widths and its creep properties by adopting proper welding methods or process. The HAZ widths and mismatches in creep properties should be fully considered in creep life assessments for the welded joints.

Doc. IIW-2572, recommended for publication by Commission X "Structural Performances of Welded Joints—Fracture Avoidance"

✉ G. Z. Wang
    gzwang@ecust.edu.cn

[1]   MOE key laboratory of Pressurized System and Safety, School of Mechanical and Power Engineering, East China University of Science and Technology, Shanghai 200237, China

1 Introduction

For defect-free welded joints at high temperature, the nucleation and propagation of voids and final type IV cracks generally occur in heat-affected zone (HAZ) due to the multiaxial stress state caused by the material constraint effect between weldment constituents and high creep deformation of soft HAZ [1]. Many experiments and theoretical evidences have been conducted to suppress type IV crack and increase the creep strength of welded joints both from microstructure approaches [2, 3] and mechanical approaches [4–6]. One of the effective methods was changing the HAZ width through employing different welding methods or processes [6–9]. Such as, the creep rupture life of electron beam (EB) and laser welds with narrower HAZ width is much longer than that of gas tungsten arc (GTA) welds with larger HAZ width for the unaxial tension welded joints at the same unaxial stress, and the fracture process and mechanism were also different for GTA welding and EB or laser welding due to the different distributions of stress triaxiality and creep strain in HAZs [6, 7]. Other evidences also show that the creep rupture life increases with decreasing HAZ width due to the lower equivalent creep strain accumulation for the narrower HAZ welds [8].

However, the cracks may inevitably be produced, and they may exist in different weldment constituents randomly or occur at any positions with different distances from the initial crack plane to the interface between different materials during the process of manufacturing, heat treatment, or in service. On the other hand, the different widths of weldment constituents will be produced for different welding methods or processes. The multiaxial stress and strain fields ahead of crack tip of initial crack plane and near the interface between different materials play an important role on creep crack growth (CCG) properties [10–12], and the different widths of the materials (such as HAZs) containing the original crack or
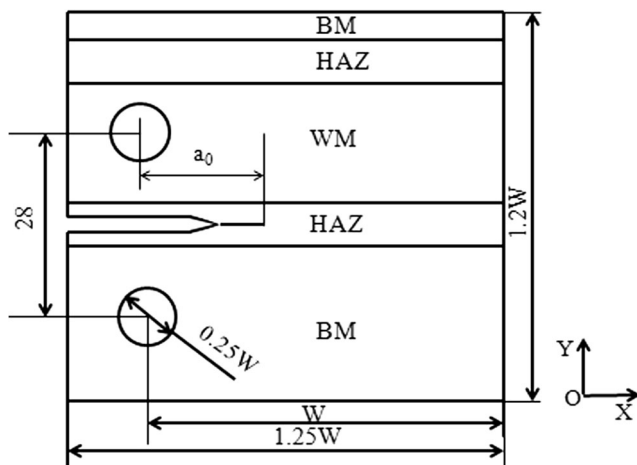
Springer

Fig. 1 The geometry and dimensions of the CT specimen of welded joint [11]

the different distance from initial crack plane to the interface between weldment constituents may lead to different multiaxial stress states around cracks due to the different material constraint effects, thus leads to different creep failure behavior and fracture properties. Such as, Tabuchi et. al [7] found that the rupture life of the EB welding with 0.5 mm HAZ width was much lower than that of GTA welding with about 2.7 mm HAZ width for P122 welded joints of compact tension (CT) specimen with pre-crack lying in the middle of HAZ at the same initial load level (this behavior is different from the defect-free welded joints). The metallurgical observation also showed that the crack located in the middle of weld metal (WM) may develop as the type IV crack due to high material constraint caused by the hard and narrow WM produced by the EB welding for P91 welded joint [13]. Similarly, a second crack also formed in the type IV region when the crack located in a hard base metal (BM) with a small distance from the initial crack plane to HAZ/BM interface for P122 welded joints [14]. All the above results show that the different widths

of the materials containing the crack or the distances from the initial crack plane to the interface between different materials affect the CCG properties. For accurate life assessment, safety design, and providing suitable guidance for welding process-es, it needs to investigate and understand this width effect on CCG behavior and creep fracture properties.

In the previous study of authors [12], it was found that when the zone containing the crack is softer than at least one of the other two surrounding materials or both, the creep crack propagates straight along the initial crack plane. Otherwise, it will form a second crack in the soft material near interface, and the time propagating in original hard materials determined the rupture life. Thus, in this paper, the finite element method (FEM) based on ductility exhaustion damage model was used to investigate the effects of HAZ widths (the distance from initial crack plane in HAZ to the interface between different materials) on CCG properties for the CT specimens with pre-crack located in the middle of softer and harder HAZs. The stress state, creep damage around cracks, rupture life, and CCG rate were calculated and analyzed, and the creep life assessment and design for welded joints were discussed.

2 Finite element models and numerical procedures

2.1 Finite element models

For investigating effects of the HAZ widths on CCG proper-ties, the CT specimen of welded joints was used for the FE analyses with ABAQUS code [15], which consists of three materials, i.e., BM, WM, and HAZ, and the HAZ width was changed. The geometry and dimensions of the CT specimen are shown in Fig. 1. The width W of the specimens is 50.8 mm, and the initial crack length a_0 is 26.4 mm (a_0/W=0.52). The width of WM is 20 mm, which is consistent with that of the

Fig. 2 The FE model of the CT specimen of welded joint with 3.2 mm HAZ width, **a** meshes of whole model, **b** local meshes around the crack tip and interfaces of HAZ/BM and HAZ/WM
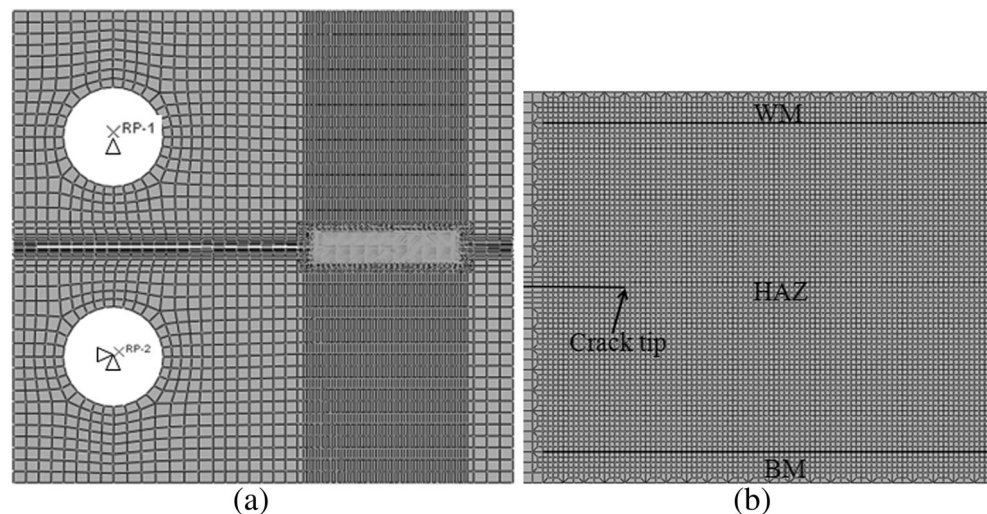

(a)   (b)

Table 1 Different configurations in creep properties of weldment constituents

Group	Configuration	MF$_{HAZ}$	MF$_W$
1	1	10	1
	2	20	1
2	3	1	5
	4	1	10
	5	1	20

experiments in Ref. [11], and the width of HAZ was changed from 0.5 to 8.0 mm. A sharp crack tip with 0.009° angle was used to represent the fatigue pre-crack and located in the middle of HAZ. The load was applied on the center of the upper hole using a reference point which was tied to the internal hole surface that represents the bolt in the experiments. The center of the upper hole was constrained in X-direction, and the center of the lower hole was constrained in X- and Y-directions. The mesh dependency in the CCG simulations has been analyzed in the literature [16, 17], and the results show that the smaller mesh size gives larger load line displacement and crack length for a given time, but the da/dt-C^* data for different mesh sizes are very similar on log-log scale. These results imply that the CCG rate is not sensitive to mesh size. Therefore, the fine meshes with size of 50×50 μm were distributed around cracks, and the four-node plane strain element (CPE4) was used for all FE models. The whole and local meshes for the typical specimen with 3.2 mm HAZ width are shown in Fig. 2, and the FE model contains 32,534 elements and 32,749 nodes.

2.2 Materials and configurations in creep properties of weldment constituents

The American Society of Mechanical Engineers (ASME) grade P92 steel was chosen for BM at 650 °C. At higher C^* and plane strain condition, plastic deformation can relax crack-tip stress and reduce CCG rate [16, 18], and the plasticity needs to be included in the CCG simulations. Thus, the elastic-plastic-creep material model was used in the FE

calculations. The elastic modulus E and yield stress σ_y of the BM is 85GPa and 126MPa at 650 °C, respectively [18]. The plastic behavior is represented by the following equation [19]:

$$\sigma = c\left(a + \varepsilon_p\right)^{\alpha} \tag{1}$$

where c, a, and α are constants (c=162, a=0.32×10^{-2}, α=0.105), and ε_p is true plastic strain. The elastic modulus and plastic behavior for WM and HAZ are assumed to be the same as those of BM. For the sake of simplicity and changing creep properties easily, the Norton's law was taken as creep constitutive equation for the three materials as follows:

$$\dot{\varepsilon}_b = A_b\sigma^{n_b}, \quad \dot{\varepsilon}_W = A_W\sigma^{n_W}, \quad \dot{\varepsilon}_{HAZ} = A_{HAZ}\sigma^{n_{HAZ}} \tag{2}$$

where $A_b, A_w,$ and A_{HAZ} are creep constants, and $n_b, n_w,$ and n_{HAZ} are creep stress exponents for BM, WM, and HAZ, respectively. The Norton's parameters (A_b=3.77E−19 $MPa^{-n}h^{-1}$, n_b=6.71) for the ASME grade P92 BM at 650 °C were used [18]. For investigating the effects of HAZ widths on CCG properties under different mismatches in creep properties, different configurations in creep properties of weldment constituents were designed. For WM and HAZ, the mismatch factor MF$_w$ (A_w/A_b) and MF$_{HAZ}$ (A_{HAZ}/A_b) were defined by varying the constant A and keeping the exponent n_w=n_{HAZ}=n_b=6.71 to represent the difference in creep strength relative to BM, respectively, which was corresponding to Ref. [12]. Five different configurations (Table 1) of MF$_W$ and MF$_{HAZ}$ were designed to investigate the effects of HAZ widths on CCG properties under the same initial load level (stress intensity factor $K = 10$ MPa.$\sqrt{m}$. For understanding the effect of the strength of the zones containing initial cracks on CCG behavior, the configurations included the conditions that the strength of HAZs containing initial cracks was lower than the other two surrounding materials (group 1: configurations 1 and 2 with softer HAZ) and higher than one of the other two materials (group 2: configurations 3, 4, and 5 with harder HAZ).

2.3 Creep damage model and crack growth simulation

The ductility exhaustion model was used to account for the creep damage accumulation and then to simulate creep crack
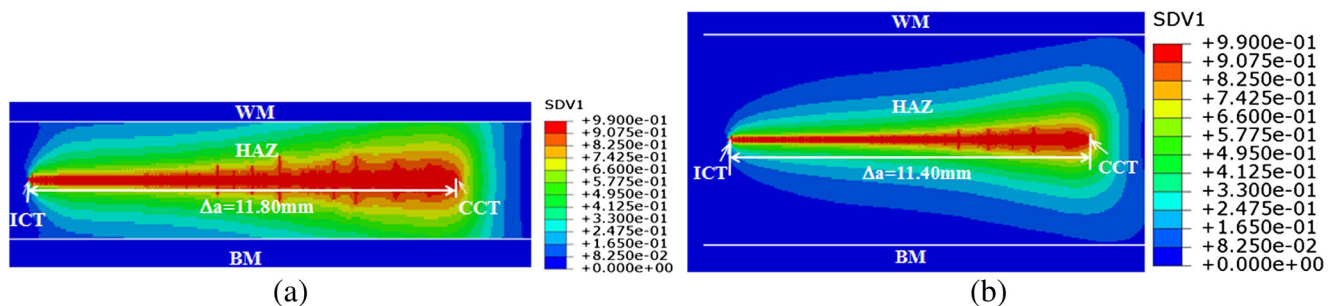

Fig. 3 The final CCG path for the specimens with different HAZ widths at the same initial load level of $K = 10$ MPa$\sqrt{m}$ for configuration 1, **a** 2.4 mm, **b** 7.0 mm, *SDV1* damage variable, *ICT* initial crack tip, *CCT* current crack tip
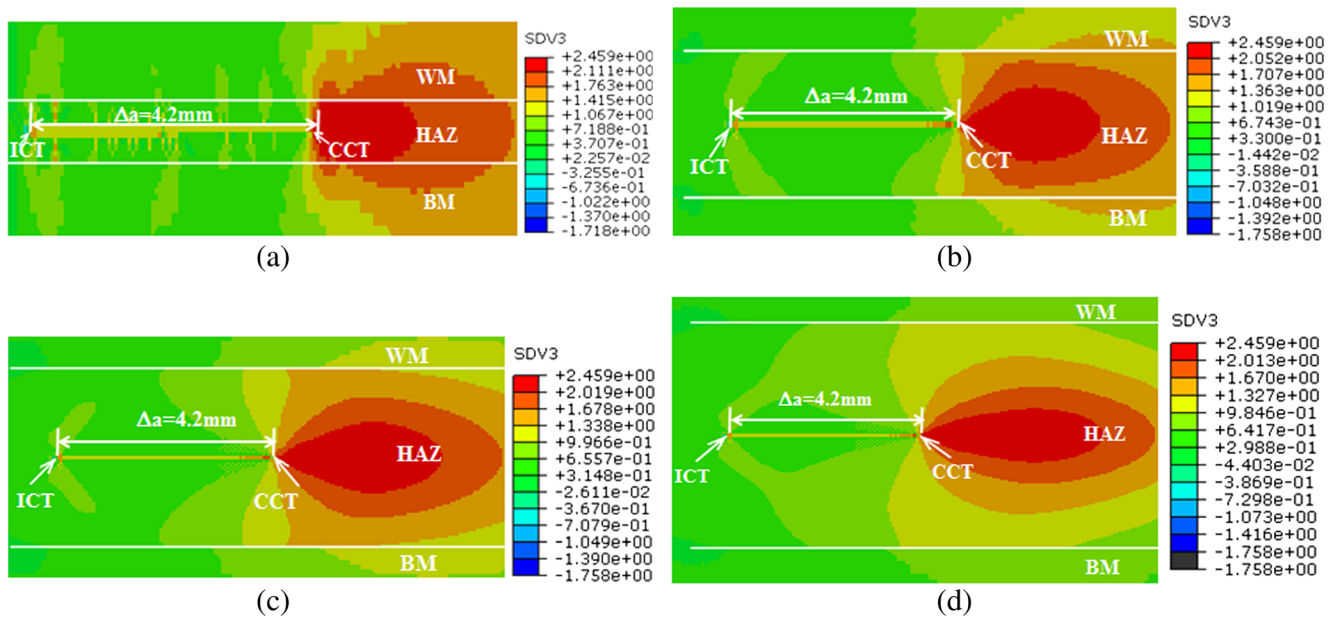
Fig. 4 The stress triaxiality contours for the specimens with different HAZ widths for configuration 4 at crack length of Δa=4.2 mm, **a** 0.5 mm, **b** 2.4 mm, **c** 4.0 mm, and **d** 7.0 mm, *SDV3* stress triaxiality, *ICT* initial crack tip, *CCT* current crack tip

growth [16–20], and the rate of damage $\dot{\omega}$ was defined by the ratio of creep strain rate $\dot{\varepsilon_c}$ and multiaxial creep ductility ε_f^* as follows:

$$\dot{\omega} = \frac{\dot{\varepsilon_c}}{\varepsilon_f^*} \qquad (3)$$

And the total damage at any instant is the integration of the damage rate in Eq. (4) up to that time [16]:

$$\omega = \int_0^t \dot{\omega}\, dt = \int_0^t \frac{\dot{\varepsilon_c}}{\varepsilon_f^*}\, dt \qquad (4)$$

where ω is the creep damage rate and $\dot{\varepsilon_c}$ and ε_f^* is the equivalent creep strain rate and multiaxial creep ductility, respectively. The value of the ω is in the range between 0 and 1. When the accumulated creep damage calculated from Eq. (5) reaches 1, local failure occurs and progressive cracking is simulated. Thus, load-carrying capacity of the point is reduced to near zero by reducing the elastic modulus to a very small

value (1 MPa in this work). The ABAQUS user subroutine USDFLD was employed to embody this failure simulation technique, and it has been widely used in the recent literatures [12, 17, 20].

It is well known that multiaxial creep ductility depends on stress triaxiality (the ratio of the mean normal stress and equivalent stress) and can be obtained from a number of available creep void growth models [21–24], but one of the notable models was proposed by Cocks and Ashby [27], given by Eq. (5):

$$\frac{\varepsilon_f^*}{\varepsilon_f} = \sinh\left[\frac{2}{3}\left(\frac{n-0.5}{n+0.5}\right)\right] \bigg/ \sinh\left[2\left(\frac{n-0.5}{n+0.5}\right)\frac{\sigma_m}{\sigma_e}\right] \qquad (5)$$

where ε_f^* and ε_f denotes the multiaxial and uniaxial creep ductility, respectively, and n is the creep exponent. For investigating the effects of HAZ widths on CCG properties and facilitating the interpretation of results, the ε_f values of the three materials were assumed to be the same, and it was taken to be 0.16 [25]. Actually, the experimental results in Ref. [25] show that the creep

Fig. 5 The Δa-t curves **a** and the change of rupture life with HAZ width **b** for the configuration 1
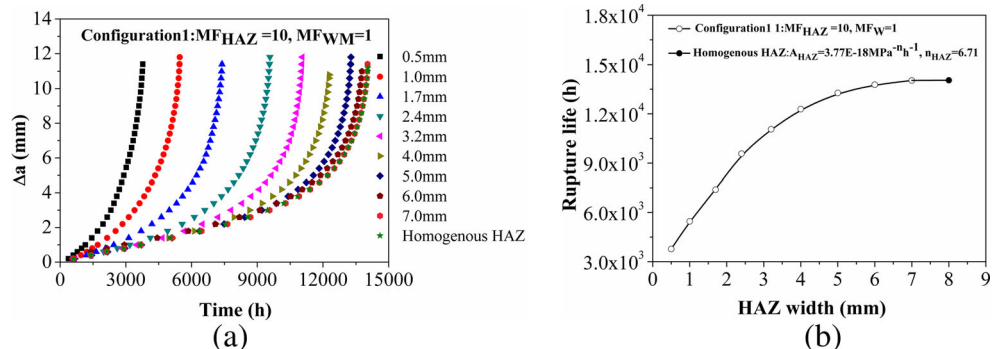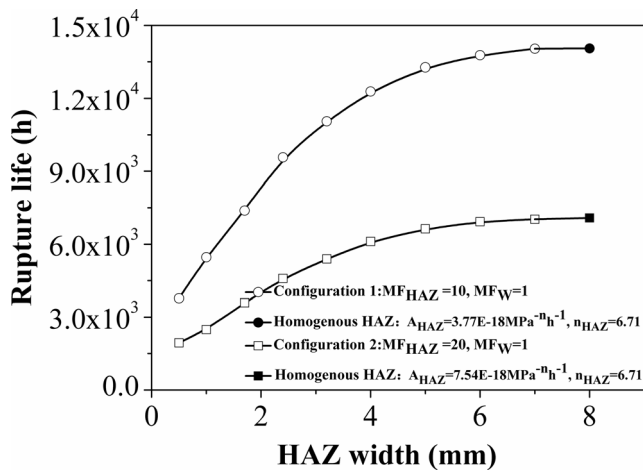
Fig. 6 The comparison of the changes of rupture life with HAZ widths for configurations 1 and 2

ductility (failure strain) of the BM, WM, and HAZ of P92 welded joints is nearly the same. The crack growth length was calculated by the number of damaged regular elements. For CT specimen of welded joints, the C* can be calculated by the following equations which consider the bending and tension in the specimen [26] and has been used in the recent literature [14, 27].

$$C^* = \frac{n}{n+1} \frac{Pd\delta/dt}{B_n(W-a)} \left(\gamma - \frac{\beta}{n} \right) \qquad (6)$$
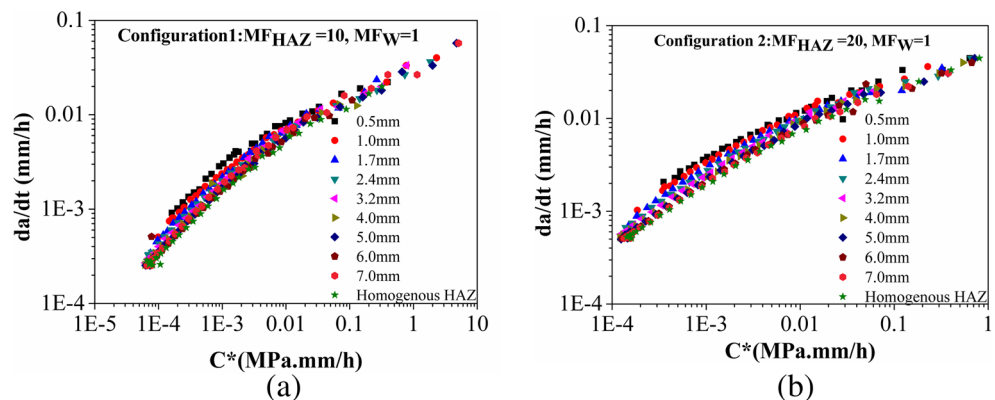
$$\gamma = \frac{2(1+\alpha)\left(1+a/W\right)(1+\alpha^2)+\alpha\left(1-a/W\right)}{\left(1+a/W\right)+\alpha\left(1-a/W\right)} \qquad (7)$$

$$\beta = \frac{\alpha}{\alpha + \left(1+a/W\right)/\left(1-a/W\right)} \qquad (8)$$

$$\alpha = \sqrt{\left\{2a/(W-a)+1\right\}^2+1} - \left\{2a/(W-a)+1\right\} \qquad (9)$$

where W is the specimen width, a is the crack length, P is the load, B_n is the net thickness of specimen, $d\delta/dt$ is the load line displacement rate, and n is the creep exponent in Norton's law.

3 Numerical results and discussions

3.1 Effect of softer HAZ width on creep crack growth properties of welded joints

In order to investigate the effect of softer HAZ width on CCG properties, the rupture life and CCG rate were calculated at nine different HAZ widths for configurations group 1 under the same initial stress intensity factor $K = 10$ MPa$\sqrt{m}$. In the previous work of authors [12], it has found that when the creep strength of the materials (HAZ) containing crack was lower than the other two surrounding materials (BM and WM), the creep crack propagates straight along the initial crack plane. Therefore, for the above configurations of group 1 (configurations 1 and 2) with softer HAZ, the cracks always propagate straight, as typically shown in Fig. 3. The SDV1 represents the damage variable, ICT is initial crack tip, and CCT is current crack tip. Figure 4 shows the stress triaxiality contours for the specimens with 0.5, 2.4, 4.0, and 7.0 mm HAZ width at the same crack growth length of Δa=4.2 mm, and SDV3 is stress triaxiality. It can be seen that the stress triaxiality ahead of crack tip decreases with increasing HAZ width due to the decrease of material constraint effect.

Figure 5 shows the crack length vs time (Δa-t) curves and the change of rupture life with HAZ width for the configuration 1, and the CCG data of homogenous HAZ specimen (A_b= 3.77E−18$MPa^{-n}h^{-1}$, n_b=6.71) was also included. It can be seen from Fig. 5 that the rupture life increases with increasing HAZ width. This is due to the higher constraint ahead of crack tip given from hard BM and WM for the specimen with narrower HAZ. This higher constraint induces higher stress triaxiality ahead of crack tips (Fig. 4) which prompts CCG; thus, the shorter rupture life is produced [28–30]. This result agrees with the experimental results of Tabuchi et.al [7] which showed that the rupture life of the EB welding with 0.5 mm HAZ width was much lower than that of GTA welding with 2.7 mm HAZ width for P122 welded joints of CT specimens with pre-crack located in the middle of HAZ at the same initial load level. It should be noted that for the three dimensional

Fig. 7 The da/dt-C* curves for specimens of group 1, **a** configuration 1, and **b** configuration 2

(a)

(b)

(3D) standard C(T) specimens in Ref.[7], the plane strain condition has been reached in a wide range of center part along crack front [31]. Thus, the result in Ref. [7] can be approximately regarded as that in plane strain condition. If the FEM analyses are conducted under plane stress condition or for 3D specimens with smaller thickness B, the results may be different from those in Fig. 5 under plane strain condition due to different Mises stress and stress triaxiality distributions ahead of crack tips. This may be related to the combining effects of out-of-plane constraint and material constraint on the CCG behavior of welded joints and needs to be further studied.

It also can be seen from Fig. 5 that the rupture life of the homogenous HAZ materials was longer than those of welded joints. Thus, the material constraint effect can decrease the CCG resistance for the welded joints with softer HAZ under the assumption that the creep failure strain does not change regardless of the creep strain rate. When the HAZ width is large enough (7 mm), the rupture life of welded joint is nearly the same with that of homogenous HAZ specimen due to the larger distance from initial crack plane to the HAZ/WM and HAZ/BM interfaces and negligible material constraint effect.

Figure 6 shows comparison of the changes of rupture life with HAZ widths for the configurations 1 and 2, and the homogenous HAZ specimen ($A_{HAZ}=7.54\text{E}-18MPa^{-n}h^{-1}$, $n_{HAZ}=6.71$) was also included. Similarly, the creep rupture life increases with increasing HAZ width for configuration 2 at $K=10\text{ MPa}\sqrt{\text{m}}$, and the rupture life of welded joints with 7 mm HAZ width was also nearly the same with that of the corresponding homogenous HAZ material. Figure 6 also shows that the rupture life of configuration 2 is shorter than that of the configuration 1 for the same HAZ width. This is due to higher creep strain accumulation caused by lower creep strength of HAZ for configuration 2. This means that increasing the creep strength of HAZ containing crack can increase the creep life of welded joints. Figure 6 also shows that the rupture life of the homogenous HAZ materials was longer than those of welded joints. This implies that the material constraint effect is detrimental for CCG properties of softer HAZs.

The relation between the CCG rate and C^* (da/dt-C^* curves) was calculated for different HAZ widths of the configurations 1 and 2, as shown in Fig. 7. Only steady state CCG data was plotted in Fig. 7. It can be seen that the CCG rate of homogenous HAZ specimens was lower than those of welded joints at a given value of C^*. The CCG rate decreases with increasing the HAZ width from 0.5 to 5 mm. After the HAZ width is larger than 5 mm, the CCG rate almost does not change. This result is consistent with that in Fig. 6 which shows that the creep rupture life increases with increasing HAZ width from 0.5 to 5 mm, and then it has very small increase with the HAZ width. The results in Figs. 6 and 7 imply that the welded joints with narrower HAZ width have shorter rupture life than those with wider ones. Figure 7 also shows that the CCG rate of $MF_{HAZ}=20$ is higher than that of
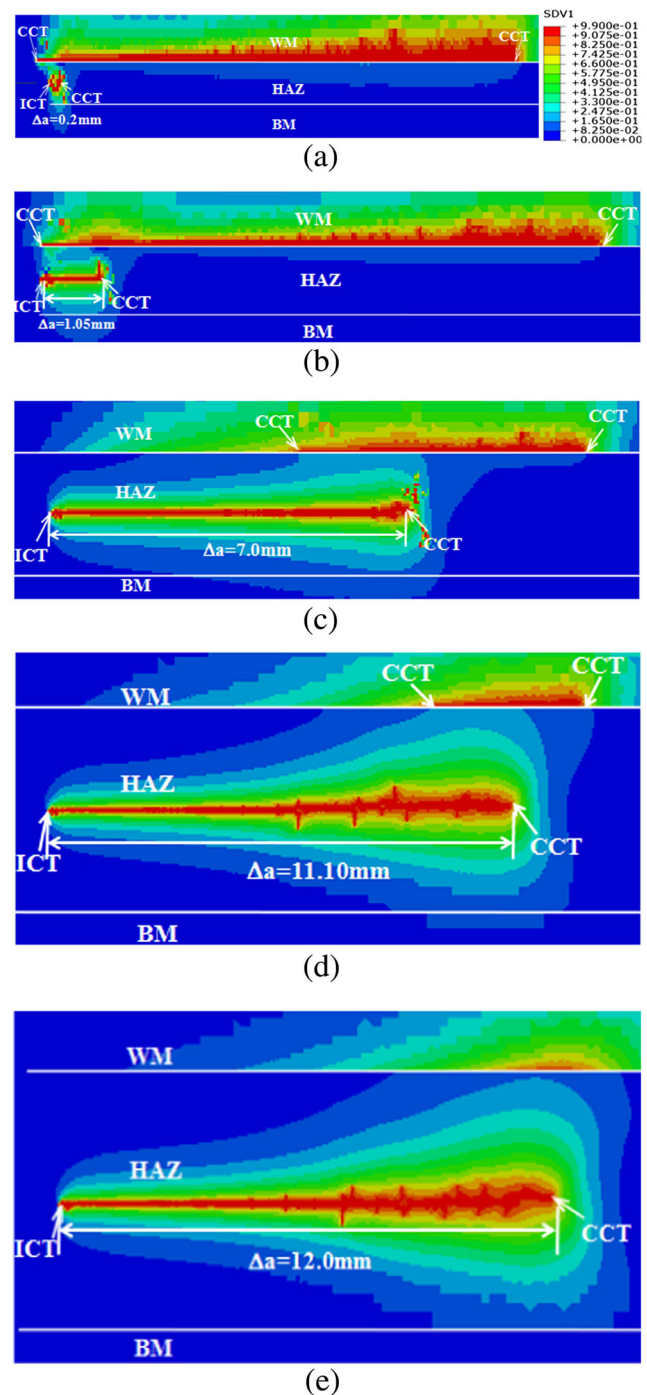

Fig. 8 The final CCG paths for the five specimens with different HAZ widths at the same initial load level of $K=10\text{ MPa}\sqrt{\text{m}}$ for configuration 4, **a** 0.5 mm, **b** 1.0 mm, **c** 2.4 mm, **d** 5.0 mm, and **e** 6.0 mm, *SDV1* damage variable, *ICT* initial crack tip, *CCT* current crack tip

$MF_{HAZ}=10$ due to the higher creep strain accumulation caused by the lower creep strength of the $MF_{HAZ}=20$ at a given value of C^*.

From all the results above for the softer HAZs, it can be concluded that the specimens with larger HAZ width (larger distance from initial crack plane to the interface between different materials) have longer rupture life and smaller CCG rate
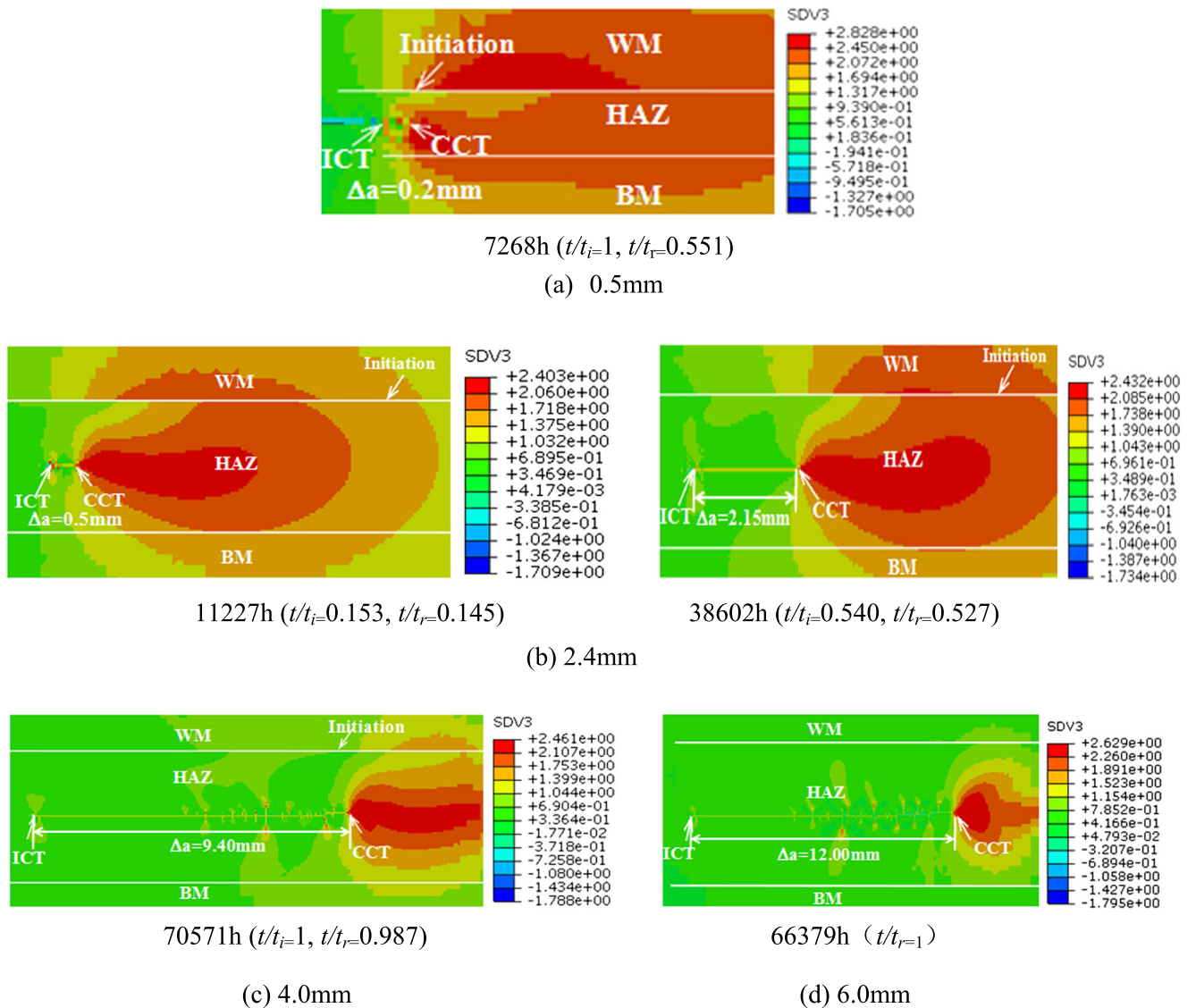
7268h (t/t_i=1, t/t_r=0.551)

(a) 0.5mm

11227h (t/t_i=0.153, t/t_r=0.145)

38602h (t/t_i=0.540, t/t_r=0.527)

(b) 2.4mm

70571h (t/t_i=1, t/t_r=0.987)

66379h（t/t_{r}=1）

(c) 4.0mm   (d) 6.0mm

Fig. 9 The stress triaxiality contours for the typical specimens with different HAZ widths for configuration 4, **a** 0.5 mm, **b** 2.4 mm, **c** 4.0 mm, and **d** 6.0 mm, *SDV3* stress triaxiality, *Initiation* the initiation location of the second crack, *ICT* initial crack tip, *CCT* current crack tip; t_i initiation time of the second crack, t_r rupture life

due to the lower material constraint effect for the wider HAZ. Thus, the designs with larger HAZ width for harder HAZ

materials containing crack can improve CCG properties and prolong life of welded joints containing crack.

Fig. 10 The Δa-t curves **a** and the change of rupture life with HAZ widths **b** for configuration 4

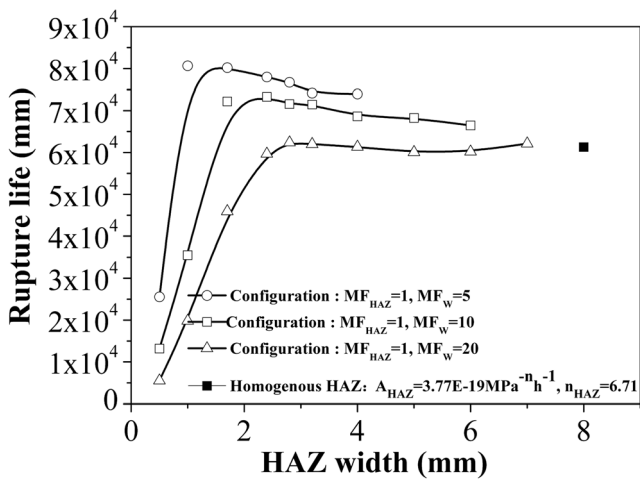
(a)   (b)
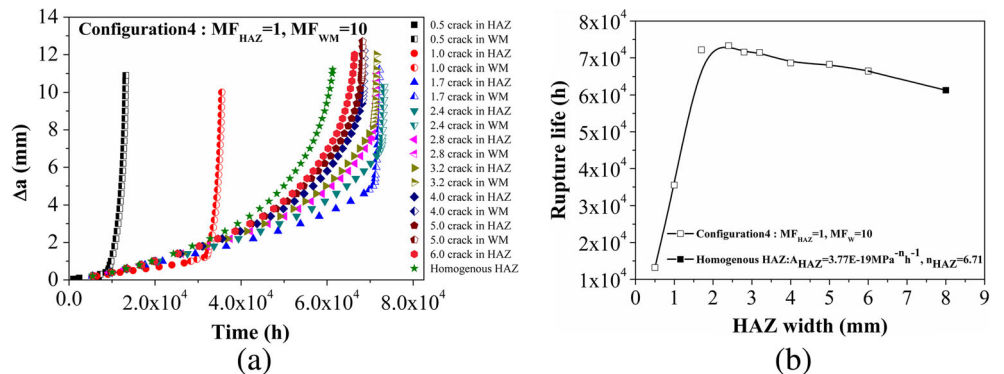
Fig. 11 The comparison of the creep rupture life of configurations 3, 4, and 5 with different HAZ widths

3.2 Effect of harder HAZ width on creep crack growth properties of welded joints

In Ref. [12], it has been shown that when the zone containing the crack was harder than one of the other two surrounding materials or both, it will form a second crack in the soft materials near interface. Thus, the crack would propagate both ahead of initial crack plane and in the soft WM near HAZ/WM interface for the specimens of group 2 (configurations 3, 4, and 5) with harder HAZ. Figure 8 shows the final damage contours and CCG paths for the typical five specimens with different HAZ widths at the same initial load level $K = 10 \mathrm{MPa}\sqrt{m}$ for configuration 4. It is interesting to note that a second crack in soft WM has formed when the HAZ width is less than or equaling 5.0 mm, and the CCG length in hard HAZ increases with increasing HAZ width. It also can be seen that the crack nearly propagates in soft WM for the specimen with 0.5 mm HAZ width, and the second crack cannot be produced for the 6.0 mm HAZ width.
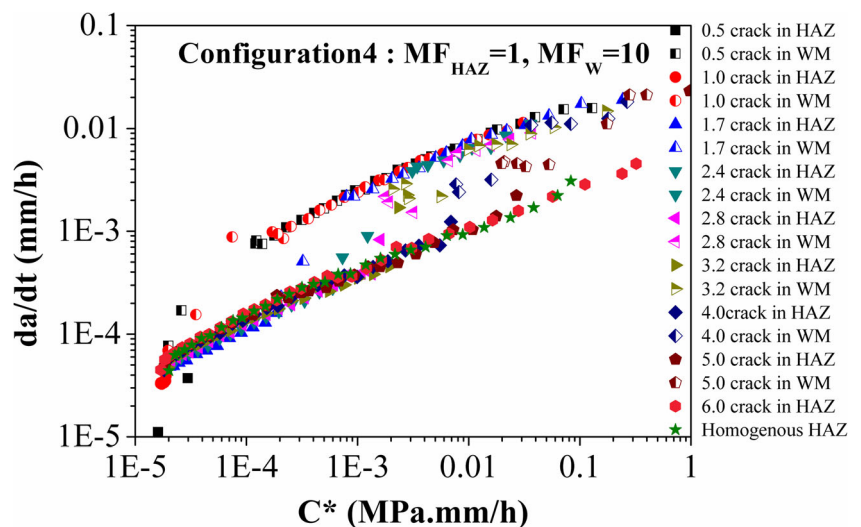
Figure 9 shows the distributions of stress triaxiality during CCG process for the typical specimens with HAZ widths of 0.5, 2.4, 4.0, and 6.0 mm. The "initiation" represents the initiation location of the second cracks, and t_i and t_r are the initiation time of the second crack and rupture life, respectively. It can be seen that the time of high stress triaxiality occurring in soft WM increases with increasing HAZ width, and the highest stress triaxiality just occurred ahead of crack tip of initial crack plane for the HAZ widths with equaling or exceeding 4.0 mm. For the specimens with narrower HAZ (0.5 and 1.0 mm), the mismatch effect in creep properties between hard HAZ and soft WM is obvious, and the strong material constraint effect leads to higher stress triaxiality in WM near WM/HAZ interface (Fig. 8a, b) after a short CCG distance. Therefore, more damage can be accumulated under high stress triaxiality in WM of WM/HAZ interface. When the damage reaches 1, the second crack would initiate in WM of interface. For the specimens with larger HAZ width (4.0 and 6.0 mm), the stress triaxiality occurring in soft WM near interface is not much higher due to smaller material constraint effect (Fig. 8c, d). Thus, the second crack initiated in soft WM after a long CCG distance in hard HAZ for the HAZ width in the range of 4.0–5.0 mm. For the 6.0 mm HAZ width, higher stress triaxiality only occurs in HAZ and the second crack cannot be produced due to negligible material constraint effect caused by the largest distance from initial crack plane to the HAZ/WM interface.

Figure 10 shows the Δa-t curves and change of rupture life with HAZ widths for configuration 4 and the data of homogenous HAZ specimen (A_{HAZ}=3.77E−19$MPa^{-n}h^{-1}$, n_{HAZ}= 6.71) is also included. It can be seen that the crack would accelerate up to fracture as soon as the second crack initiates in welded joints; therefore, the time of CCG in hard HAZ determines the rupture life. This is consistent with the result in Ref. [12]. With increasing the HAZ width from 0.5 to about 2.0 mm, the rupture life increases due to the decrease of stress

Fig. 12 The da/dt-C^* curves for welded joints with different HAZ widths for configuration 4

triaxiality (Fig. 9b) and the later initiation of second cracks, and then, it slightly decreases with the HAZ width due to gradual loss of the beneficial effect of material constraint (the effect of decreasing stress triaxiality) for the specimens with harder HAZ. It can also be seen that the rupture life of homogenous specimen was longer than those of welded joints with 0.5 and 1.0 mm HAZ width, but it was lower than those of welded joints with equaling or exceeding 1.7 mm HAZ width. This implies that the material constraint effect is beneficial for improving CCG properties for wider and harder HAZs.

The Δa-t curves for different HAZ widths for configurations 3 and 5 are similar to those of Fig. 10a. The CCG length propagating in hard HAZ increases with increasing HAZ width for these two configurations, and it cannot form the second cracks in soft WM when the HAZ width reaches 5.0 and 8.0 mm for configurations 3 and 5, respectively. Figure 11 shows the comparison of the changes of rupture life with HAZ widths for the configurations 3, 4, and 5. It can be seen that the curves of the configurations 3 and 5 are similar to that of the configuration 2 in Fig. 10b. With increasing MF_W (decreasing creep strength of WM) for the same HAZ width, the rupture life decreases due to the earlier creep crack initiation and propagation in the WM with lower creep strength.

Figure 12 shows the da/dt-C^* curves for the welded joints with different HAZ widths for configuration 4. It can be seen that the CCG rate becomes much higher in soft WM near interface than that in original hard HAZ, which is consistent with the results in Ref. [12]. The HAZ widths have less effect on the CCG rates in harder HAZ and softer WM, and the difference in rupture life for different HAZ widths mainly arise from the initiation time of the second cracks due to the material constraint effects. The da/dt-C^* curves of the configurations 3 and 5 are similar to those of the configuration 4 in Fig. 12.

From all the results above, it can be concluded that it would form a second crack in soft materials near interface between hard and soft materials for the cracks located in harder HAZ, when the distance from initial crack plane to the interface was not too large. Otherwise, the crack would propagate straight along initial crack plane. There exist the proper widths of the HAZ containing the crack which have the longest rupture life due to the lower stress triaxiality and later initiation of second crack in soft materials near interface. The CCG properties of HAZs may be improved by adjusting HAZ widths and its creep property by adopting proper welding methods or process.

3.3 Considerations of HAZ widths and mismatch effects in creep life design and assessment for welded joints

From the results above, it can be seen that the specimens with different HAZ widths have different rupture life and CCG rate

under the same load level, and the mismatch effects in creep properties also influence the rupture life and CCG rate for the specimens with the same HAZ width. Therefore, the HAZ widths and mismatch effect should be fully considered in creep life design and assessment for the welded joints. From Figs. 6 and 11, it can be concluded that the proper designs of HAZ width and mismatch in creep properties between weldment constituents can lead to longer rupture life.

On the other hand, if the CCG rate data of homogenous materials are used in creep life assessment for HAZ cracks with different HAZ widths and HAZ creep properties, the conservative or non-conservative results may be produced. Figure 11 shows that if the CCG data of welded joints with narrower HAZ width (0.5 mm) are used for the components with larger HAZ width (5 and 6 mm), the conservative results will be produced for harder HAZ specimen, while the non-conservative results will be produced inversely. Thus, the actual CCG data for the specimens with different HAZ widths and mismatches in creep properties should be obtained by experiments or FE simulations and used in creep life assessment of welded joints with HAZ cracks.

4 Conclusion

The finite element method (FEM) based on ductility exhaustion damage model was used to investigate the effects of HAZ widths (the distance from initial crack plane to the interface between different materials) on CCG properties for the CT specimens of welded joints with pre-crack located in the middle of softer and harder HAZs under the same initial load level. The stress state, creep damage around cracks, rupture life, and CCG rate were calculated and analyzed, and the creep life assessment and design for welded joints were discussed. The main results obtained are as follows:

1. For the welded joints with softer HAZ containing crack, the crack always propagates straight, and the material constraint effect is detrimental for CCG properties. The creep rupture life increases and CCG rate decreases with increasing HAZ width due to the decrease of material constraint effect. The designs with wider HAZ containing crack can improve CCG properties and prolong life of welded joints with softer HAZs.

2. For the welded joints with harder HAZ containing crack, a second crack in soft WM near interface generally forms during creep crack growth in harder HAZ, and the rupture life is mainly determined by the initiation time of the second crack. The CCG length in harder HAZ increases with increasing HAZ width. The material constraint effect is beneficial for improving CCG properties for wider and harder HAZs. There exist proper widths of the harder HAZ which have the longest rupture life due to the lower

stress triaxiality and later initiation of second crack in soft WM near interface.

3. The CCG properties of HAZs may be improved by adjusting HAZ widths and its creep property by adopting proper welding methods or process.

4. The HAZ widths and mismatches in creep properties should be fully considered in creep life design and assessment for the welded joints. The actual CCG rate data for the specimens with actual HAZ widths and mismatches should be obtained by experiments or FE simulations and used in creep life assessment of welded joints.

References

1. Abe F, Tabuchi M, Tsukamoto S, Shirane T (2010) Microstructure evolution in HAZ and suppression of type IV fracture in advanced ferritic power plant steels. Int J Press Vessels Pip 87:598–604

2. Abe F, Tabuchi M, Kondo M (2006) Suppression of type IV fracture in welded joints of advanced ferritic power plant steels-effect of boron and nitrogen. Mater High Temp 23:145–154

3. Kimura K, Sawada K, Kushima H, Toda Y (2013) Influence of chemical composition and heat treatment on long-term creep strength of grade 91 steel. Procedia Eng 55:2–9

4. Hyde TH, Sun W, Becker AA (2004) Effect of geometry change on the creep failure life of a thick-walled CrMoV pipe with a circumferential weldment. Int J Press Vessels Pip 81:363–371

5. Mayr P, Mitsche S, Cerjak H, Allen SM (2011) The impact of weld metal creep strength on the overall creep strength of 9% Cr steel weldments. J Eng Mat Tech 113(2): 21011(1–7)

6. Albert SK, Tabuchi M, Hongo H, Watanabe T, Kubo K, Matsui M (2005) Effect of welding process and groove angle on type IV cracking behavior of weld joints of a ferritic steel. Sci Technol Weld Joining 10:149–157

7. Tabuchi M, Watanabe T, Kubo K, Matsui M, Kinugawa J, Abe F (2001) Creep crack growth behavior in HAZ of weldments of W containing high Cr steel. Int J Press Vessels Pip 78:779–784

8. Zhao L, Jing HY, Xu LY, An JC, Xiao GC (2012) Numerical investigation of factors affecting creep damage accumulation in ASME P92 steel welded joint. Mater Des 34:566–575

9. Li D, Shinozaki K, Kuroki H (2003) Stress-strain analysis of creep deterioration in heat affected weld zone in high Cr ferritic heat resistant steel. Mater Sci Technol 19:1253–1260

10. Kim WG, Park JY, Lee HY, Hong SD, Kim YW, Kim SJ (2013) Time-dependent crack growth behavior for a SMAW weldment of Gr. 91 steel. Int J Press Vessels Pip 110:66–71

11. Sugiura R, Yokobori AT Jr, Suzuki K, Tabuchi M (2010) Characterization of incubation time on creep crack growth for weldments of P92. Eng Fract Mech 77:3053–3065

12. Chen G, Wang GZ, Xuan FZ, Tu ST (2014) Mismatch effect in creep properties on creep crack growth behavior. Mater Des 63: 600–608

13. Dogan B (2007) Creep deformation and failure assessment of steel weldments. Eighth international conference on creep and fatigue at elevated temperatures, San Antonio, Texas, USA.

14. Tabuchi M, Hongo H, Watanabe T, Yokobori AT Jr (2007) Creep crack growth analysis of welded joints for high Cr heat resisting steel. ASTM Spec Tech Publ 1480:93–101

15. ABAQUS (2012) in version 6.10, SIMULIA

16. Yatomi M, Nikbin K, O'Dowd NP (2003) Creep crack growth prediction using a damage based approach. Int J Press Vessels Pip 80:573–583

17. Oh CS, Kim NH, Kim YJ, Davies C, Nikbin K, Dean D (2011) Creep failure simulations of 316H at 550°C: part I—a method and validation. Eng Fract Mech 78:2966–2977

18. Yatomi M, Tabuchi M (2010) Issues relating to numerical modelling of creep crack growth. Eng Fract Mech 77:3043–3052

19. Sugiura R, Yokobori JAT, Tabuchi M, Yokobori T (2007) Comparison of creep crack growth rate in heat affected zone of welded joint for 9%Cr ferritic heat resistant steel based on C^*, $d\delta/dt$, K and Q^* parameters. Eng Fract Mech 74:868–881

20. Kim NH, Oh CS, Kim YJ, Davies C, Nikbin K, Dean D (2013) Creep failure simulations of 316H at 550°C: part II—effects of specimen geometry and loading mode. Eng Fract Mech 1059: 169–181

21. Spindler MW (2004) The multiaxial creep ductility of austenitic stainless steels. Fatigue Fract Eng Mater Struct 27:273–281

22. Manjoine MJ (1982) Creep rupture behavior of weldments. Weld J 61:50–57

23. Rice JR, Tracey DM (1969) On ductile enlargement of voids in traxial stress fields. J Mech Phys Solids 17(3):201–217

24. Cocks ACF, Ashby MF (1980) Intergranular fracture during power-law creep under multiaxial stresses. Metal Sci 14:395–402

25. Zhao L, Jing HY, Han YD, Xiu JJ, Xu LY (2012) Prediction of creep crack growth behavior in ASME P92 steel welded joint. Comput Mater Sci 61:185–193

26. ASTM, ASTM STP 791 (1983) Unified solution for J ranging continuously from pure bending to pure tension. Fracture Mechanics, pp. 499–519

27. Tabuchi M, Yokobori AT Jr, Sugiura R, Yatomi M, Fuji A, Kobayashi K (2010) Results of a Japanese round robin program for creep crack growth using Gr.92 steel welds. Eng Fract Mech 77: 3066–3076

28. Wang GZ, Liu XL, Xuan FZ, Tu ST (2010) Effect of constraint induced by crack depth on creep crack-tip stress field in CT specimens. Int J Solids Struct 47:51–57

29. Sun PJ, Wang GZ, Xuan FZ, Tu ST, Wang ZD (2011) Quantitative characterization of creep constraint induced by crack depths in compact tension specimens. Eng Fract Mech 78:653–665

30. Wang GZ, Li BK, Xuan FZ, Tu ST (2012) Numerical investigation on the creep crack-tip constraint induced by loading configuration of specimens. Eng Fract Mech 79:353–362

31. Sun PJ, Wang GZ, Xuan FZ, Tu ST, Wang ZD (2012) Three-dimensional numerical analyses of out-of-plane creep crack-tip constraint in compact tension specimens. Int J Press Vessels Pip 96–97:78–89